

Piezoelectric Ceramics Nonlinear Behavior. Application to Langevin Transducer

D. Guyomar, N. Aurelle (*) and L. Eyraud

Laboratoire Génie Électrique et Ferroélectricité, Bâtiment 504, INSA Lyon,
20 avenue Albert Einstein, 69621 Villeurbanne Cedex, France

(Received 2 July 1996, revised 30 September 1996, accepted 28 November 1996)

PACS.43.25.-x – Nonlinear acoustics, macrosonics

PACS 43.38.-p – Transduction; acoustical devices for the generation
and reproduction of sound

PACS.43.30.-k – Underwater sound

Abstract. — Drastic behavior changes occur for power transducers using PZT type of ceramics. A better characterization under high excitations is then required for piezoelectric materials. Indeed, characteristic nonlinear behaviors such as resonance frequency shift with hysteresis effect and overtones generation are observed experimentally. They result in front mass displacement saturation, drop in performances and instabilities. To interpret such features, a nonlinear approach is proposed. This resulting nonlinear model has been applied to the transducer and simulations are given. The comparison between numerical simulations and experimental results shows good agreement. Usually, observed saturation effects are interpreted as in term of viscous factor increase, our nonlinear approach gives an alternative explanation that explains also others observed phenomena.

Résumé. — Des changements importants de comportement sont observés sur des transducteurs de puissance utilisant des céramiques de type PZT. Une meilleure caractérisation des matériaux piézoélectriques sous hauts niveaux s'avère alors nécessaire. En effet, des phénomènes caractéristiques d'un comportement non linéaire tels que le décalage de la fréquence de résonance avec hystérésis ou la génération d'harmoniques ont été observés expérimentalement. Ceci se traduit par des effets de saturation du niveau de déplacement de la face avant, une limitation des performances du système et un fonctionnement instable. Afin d'interpréter de tels comportements, une théorie non linéaire est proposée. Ce modèle a ensuite été appliqué à notre structure de transducteur. Une comparaison entre simulations et résultats expérimentaux a permis de valider cette nouvelle approche. Les effets de saturation observés ont été jusqu'à présent toujours reliés à la variation du coefficient d'amortissement, notre étude a permis de démontrer qu'une autre explication liée aux non linéarités était possible et permettait en même temps d'expliquer d'autres phénomènes observés

(*) Author for correspondence (e-mail: naurelle@ge-serveur.insa-lyon.fr).

1. Introduction

Piezoelectric ceramics, used in power transducers for sonars, ultrasonic welding or cleaning systems, are often subjected to high mechanical and electrical drives. Thus, nonlinear working domains are rapidly reached for these materials and the classical linear approach is no longer sufficient to interpret experimental results.

Actually, in most problems of elasticity, the relations given between two parameters are linear in a first approach. The linearization is assumed to be valid in a small motion hypothesis which is no more convenient for large amplitude motions [1-4].

Nowadays, piezoelectricity has to cope with nonlinear problems that must be solved for power applications. In this paper, first we present the nonlinearities induced in power transducer. Then we propose a theoretical piezoelectric nonlinear model that we apply to our test structure. We will not use the standard Mason model but rather a mechanical lumped model for our transducer. Finally, a simulation work has been achieved to compare our nonlinear theory prediction with experimental results.

2. Experimental Nonlinear Phenomena

To study the piezoelectric ceramic behavior under high mechanical excitations, we chose to work on a prestressed symmetrical Langevin transducer, made up of four power ceramic rings (P189 from Quartz & Silice company - France) and two tail masses. Experimentation has been made in air at the resonant frequency of the transducer, consequently low electrical fields have been applied to the ceramics (*cf.* Fig. 1). A low distortion signal is generated by the HP3577A analyzer and then amplified with the NF4505. This equipment presents high rejection level. However to make sure that the nonlinearities are really generated in the ceramics, we have run experiments on pure resistive load instead of the transducer. On the pure resistive load, under driving levels equivalent to the ones used for the transducer, the harmonics to fundamental ratio was below 40 dB. Besides, a stress sensor, made out of two thin disks of P189 ceramic with opposite poling, can be inserted in the middle of the piezostack to record the stress waveform. One of the first observation is the resonance frequency shift towards the low frequencies that appears when increasing the excitation level. An hysteresis effect is also noticed whether the frequency is swept in increasing or decreasing mode [5, 6].

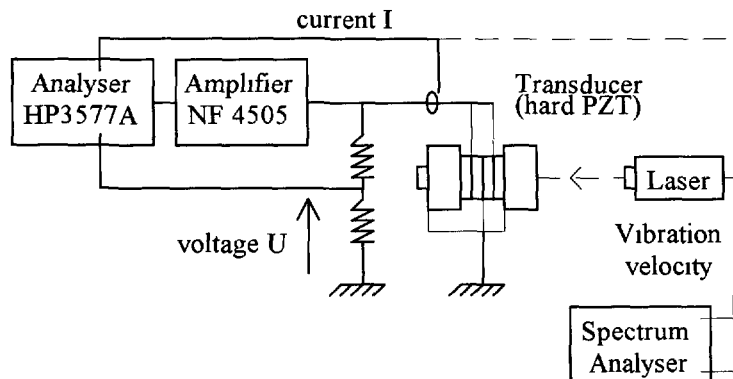


Fig. 1 — Experimental set-up

Moreover, when the electrical excitation level is sufficient enough, a distinct distortion appears on the current, velocity, stress or power signals (*cf.* Figs. 2, 3, 4)

This distortion effect corresponds, in the Fourier domain, to a spectrum that presents a ray structure due to the harmonics and subharmonics (*cf.* Fig. 5). We note, for high excitation levels, a sudden period doubling appearance ($f/2$).

When increasing the input voltage, the energy transfer from the fundamental to the harmonics results in an amplitude saturation of the displacement and current.

3. Model

To describe the nonlinear behavior of the piezoelectric ceramics, we extend up to the second order the constitutive piezoelectric equations, around the prestressed static state (T_0, D_0). Indeed we introduce new nonlinear piezoelectric coefficients [7, 8]. Then, thanks to thermodynamic relationships, the number of independent coefficients has been reduced, subsequently the stress T and induction D can be expressed as:

$$\begin{aligned} T &= T_0 + cS - eE + \frac{\alpha S^2}{2} + \frac{\beta E^2}{2} - \gamma SE \\ D &= D_0 + eS + \varepsilon E + \frac{\gamma S^2}{2} + \frac{\delta E^2}{2} - \beta SE \end{aligned} \tag{1}$$

where S is the strain, E the electrical field, c, e, ε the classical linear piezoelectric coefficients and $\alpha, \beta, \gamma, \delta$ the new nonlinear ones. Afterwards, on the assumption that there is no coupling between dynamic and static states, the terms T_0 and D_0 will not be considered and weakly nonlinear equations will be obtained.

As we work at the resonant frequency in the air, the electrical fields applied are low. Therefore, in the following calculations, we do not take into account the nonlinearities due to electrical field. Our transducer can be regarded as a mass-spring system in a low frequency regime (the wavelength is such larger than the piezostack length), so we can write:

$$M \frac{\partial^2 u}{\partial t^2} = -T\Sigma \tag{2}$$

where M is the mass, Σ the ceramic ring surface and u the front mass displacement. We make sure that the displacement of the piezostack and the displacement on the mass are equivalent so as to consider the front mass as a rigid mass.

Substituting in this last equation the nonlinear expression of the stress T , the strain S by the ratio u/l (l : half length of the piezostack) and adding up a damping term in λ , we get the nonlinear oscillator equation:

$$\frac{\partial^2 u}{\partial t^2} + w^2 u + \alpha_1 u^2 - \frac{\gamma \Sigma}{lM} uE + 2\lambda w \frac{\partial u}{\partial t} = \frac{e \Sigma}{M} E, \tag{3}$$

where w is the eigenpulsation of the transducer:

$$\frac{c \Sigma}{lM} = w^2, \quad \frac{\alpha \Sigma}{2l^2 M} = \alpha_1, \quad \text{and} \quad \lambda = \frac{\lambda_1 \Sigma}{2wlM}.$$

In the first experimental part, we noticed that the vibration speed signal is distorted but remains periodic, consequently the displacement u can be expressed as a Fourier sum:

$$u(t) = \sum_{n=-\infty}^{n=+\infty} c_n e^{jn\Omega t}, \tag{4}$$

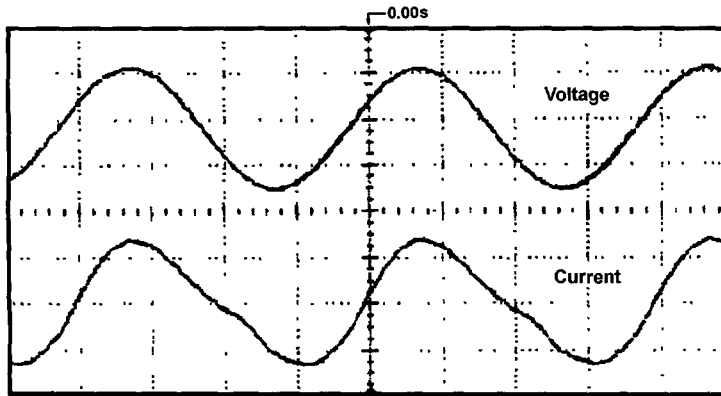


Fig. 2 — Voltage and current signals (Transducer P189/40 MPa/65 Vpeak).

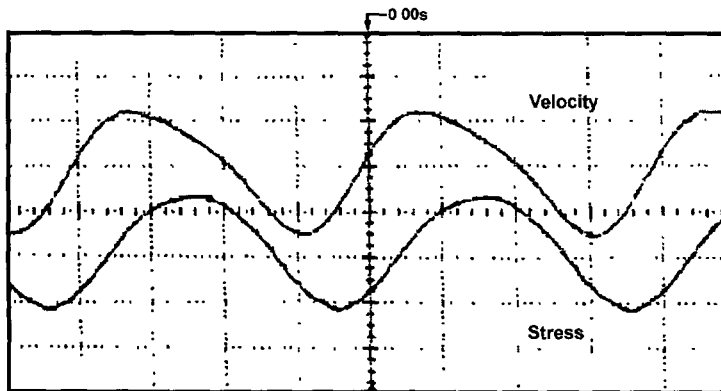


Fig. 3 — Stress and velocity signals (Transducer P189/40 MPa/65 Vpeak).

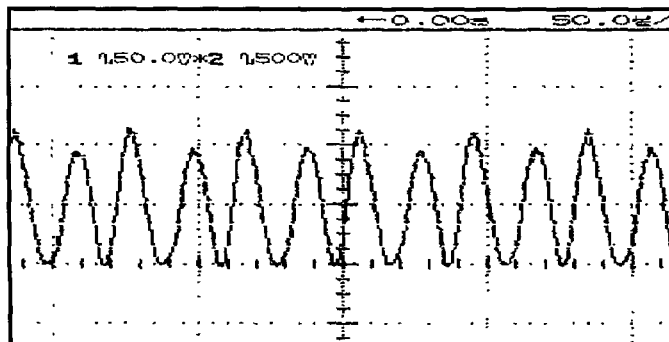


Fig. 4. — Electrical power signal (Transducer P189/40 MPa/65 Vpeak).

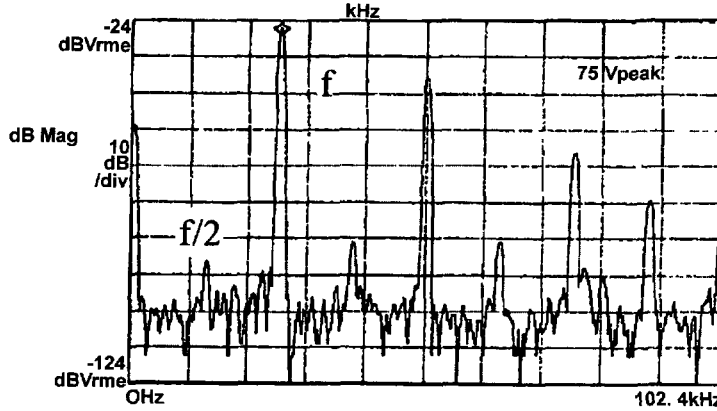


Fig. 5. — Current spectrum (Transducer P189/40 MPa/75 Vpeak).

where Ω is the variable excitation signal pulsation, that is to say the electrical field pulsation:

$$E(t) = \frac{E_0}{2} (e^{j\Omega t} + e^{-j\Omega t}), \quad (5)$$

where E_0 is the electrical field peak value.

These previous expressions can be inserted in equation (3), it gives:

$$\begin{aligned} & - \Omega^2 \sum_{n=-\infty}^{n=+\infty} n^2 c_n e^{jn\Omega t} + w^2 \sum_{n=-\infty}^{n=+\infty} c_n e^{jn\Omega t} + \alpha_1 \sum_{n=-\infty}^{n=+\infty} \sum_{m=-\infty}^{m=+\infty} c_n c_m e^{j(n+m)\Omega t} \\ & - \frac{\gamma \Sigma E_0}{2lM} \left(\sum_{n=-\infty}^{n=+\infty} c_n e^{j(n+1)\Omega t} + \sum_{n=-\infty}^{n=+\infty} c_n e^{j(n-1)\Omega t} \right) \\ & + 2\lambda w j \Omega \sum_{n=-\infty}^{n=+\infty} n c_n e^{jn\Omega t} = \frac{e \Sigma E_0}{2M} (e^{j\Omega t} + e^{-j\Omega t}). \end{aligned} \quad (6)$$

This equation holds for each frequency $k\Omega$ (k : positive integer), it gives the modulus and phase of the coefficients c_n , that correspond to the displacement amplitudes for each frequency. The resolution has been made until the frequency 3Ω ($n = 3$).

The same calculations can be transposed for the induction equation (D). They give the current amplitudes evolution, corresponding to the fundamental and harmonics frequencies, for different driving levels (E_0) or different driving frequencies (Ω).

4. Simulation Results and Comparison with Experimental Results

Simulations of displacement or current nonlinear equations, previously described, have been made and have permitted an evaluation of the nonlinear coefficients. The following convention: $T > 0$ and $S > 0$ for compression, although not standard, was adopted. The damping coefficient λ is evaluated from the transducer quality factor measurement. A first evaluation of the nonlinear coefficients is made with the curves representing the strain *versus* the stress in the static regime. Then, a better fit around this initial guess is made to adjust the displacement

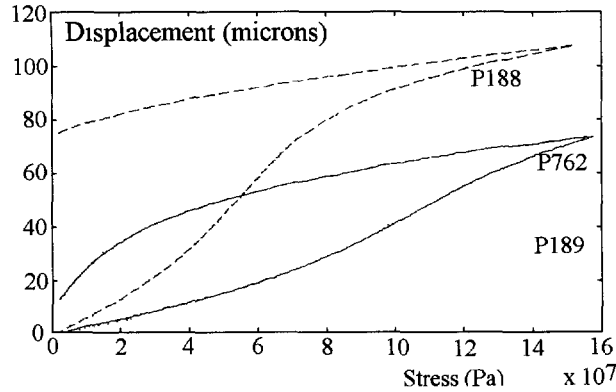


Fig 6. — Curve: displacement = $f(\text{static stress})$. Experimentation has been made on ceramic rods whose dimensions are $\phi = 6.35 \text{ mm}$, $L = 15 \text{ mm}$

and current experimental curves over a large range of voltage. The simulation results displayed below have been obtained with the following parameters set:

$$\begin{array}{ll}
 w = 2\pi \times 27\,000 \text{ Hz} & \lambda = 0.0015 \text{ N s}^2 \text{ m}^{-1} \text{ kg}^{-1} \\
 \Sigma = 8 \times 10^{-5} \text{ m}^2 & \alpha_1 = -1.55 \times 10^{15} \text{ N m}^{-2} \text{ kg}^{-1} \\
 l = 6.6 \times 10^{-3} \text{ m} & \gamma = -2.8 \times 10^4 \text{ N m}^{-1} \text{ V}^{-1} \\
 M = 20 \times 10^{-3} \text{ kg} & \beta = 6 \times 10^{-5} \text{ N V}^{-2}.
 \end{array}$$

Note. — The relationship between strain and stress in the static regime in the compression mode are given in Figure 6 [9]. The variation of the static compliance s_{33}^E function of the applied stress can then be deduced. We can see from these curves that the s_{33}^E coefficient increases with the compressive stress, or that the c_{33}^E coefficient decreases. With our sign convention and to keep a continuity between static and dynamic modes, the nonlinear coefficient α has to be negative to explain a decrease of the c_{33}^E coefficient in compression. Indeed, it can be written:

$$T = \left(c + \frac{\alpha S}{2}\right)S - eE - \gamma SE$$

First, simulation runs allow to describe the resonance frequency shift that is due to the nonlinear term α that modifies the material elasticity with the strain level.

For low driving levels, nonlinearities are of low influence and the displacement amplitude evolution is a symmetrical curve whose maximum is located at the system eigenfrequency (w) (*cf.* Fig. 7).

When the excitation level increases, the solution obtained for equation (6) when $n = 1$ (fundamental frequency) consists of three real solutions for a particular frequency domain (*cf.* Fig. 7), defined by the condition $\frac{d|C_1|}{dw} \Rightarrow \infty$. In this case, the hysteresis phenomenon appears.

It can be shown that the AC part is unstable, therefore the amplitude cannot venture in this zone. It results in an amplitude and phase jumps from A to B and C to D. (*cf.* Fig. 8). As a consequence the transducer exhibits a different resonant frequency for a upgoing or downgoing frequency sweep.

These hysteresis or resonance frequency shift increase with the driving signal. Consequently, for high driving levels, the experimental measurement of the quality factor Q_m becomes difficult and badly defined.

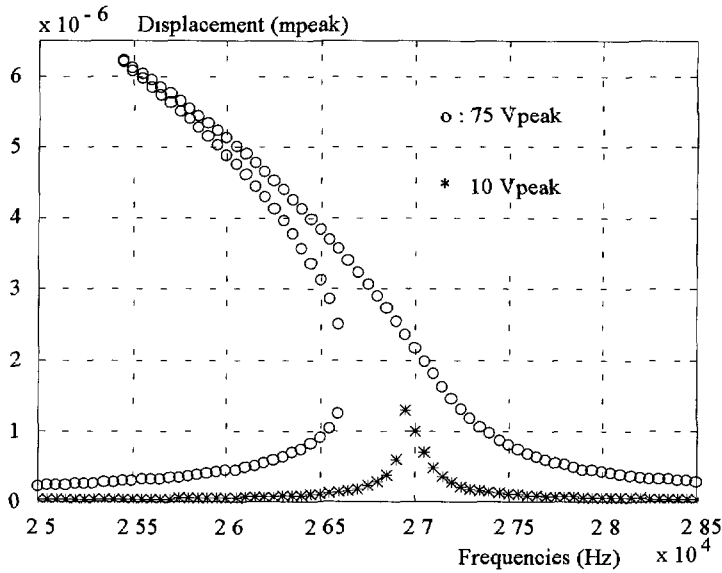


Fig 7. — Simulated displacement curves.

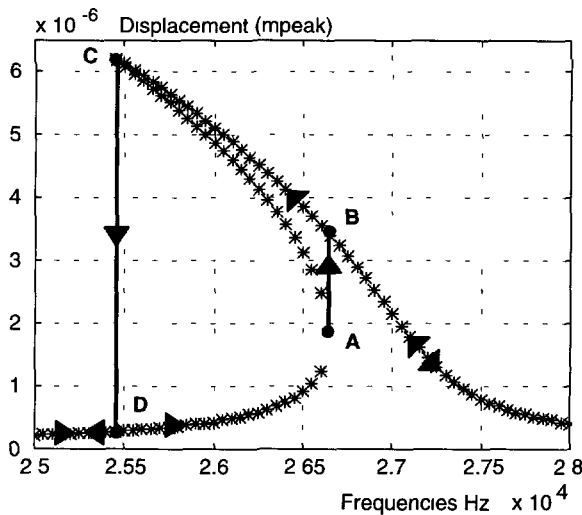


Fig. 8. — Hysteresis phenomenon simulation

In Figure 9, the time waveforms of current, displacement, velocity and stress are reconstructed from Fourier series, the apparent distortion on these simulated signals are quite similar to the observed ones (*cf.* Fig. 9 and Figs. 2-3).

The amplitudes corresponding to the fundamental resonant frequency f (where a maximum of current is reached) and to the first harmonic $2f$ of the current and displacement signals are represented for different excitation levels (*cf.* Figs. 10, 11). A saturation effect appears on these curves. The displacement amplitude shows a drop of 40%, for a driving signal of 75 Vpeak/3 mm, with regard to the linear behavior.

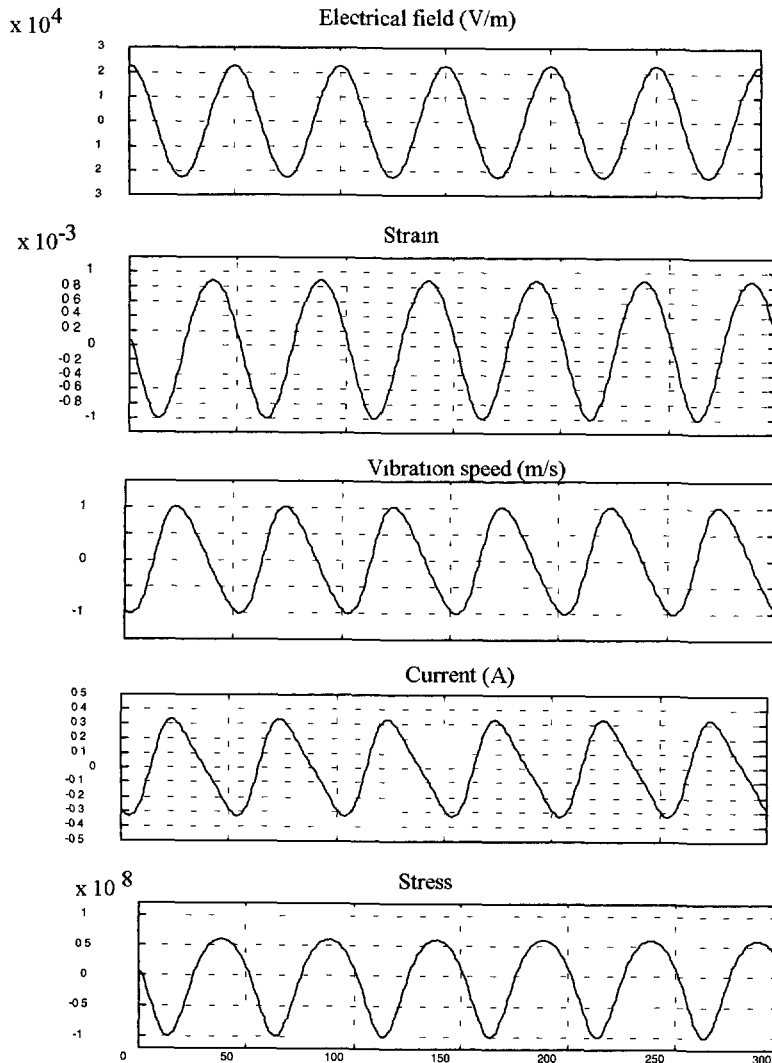


Fig. 9. — Simulated time signals for resonance working condition $75 \text{ V}_{\text{peak}}/\text{time step} = 1/(50.25000) \text{ s}$ (50 dots per period/the resonant frequency is around 25 000 Hz for highest levels).

Simulations show also the influence of the nonlinear term γ on the displacement amplitude: the higher the nonlinearity γ in SE is, the smaller the deformation amplitude is. Besides, the electromechanical factor “ N ”, defined in the Mason model as the transformer ratio, decreases when the applied electrical field is increased (*cf.* Fig. 12). This effect explains that the electromechanical conversion has a smaller efficiency for high excitations. Computing from the nonlinear mode the electromechanical conversion coefficient N shows that this coefficient drops with the applied electrical field. The piezoelectric conversion is lower at high driving amplitude, thus explains the saturation effects.

The simulated plot $T = f(S)$ shows a different behavior of the ceramic working in the compressive or extension mode (*cf.* Fig. 13). The piezoelectric model chosen at the beginning implies a material hardening in the expansion mode and a material softening in the compressive

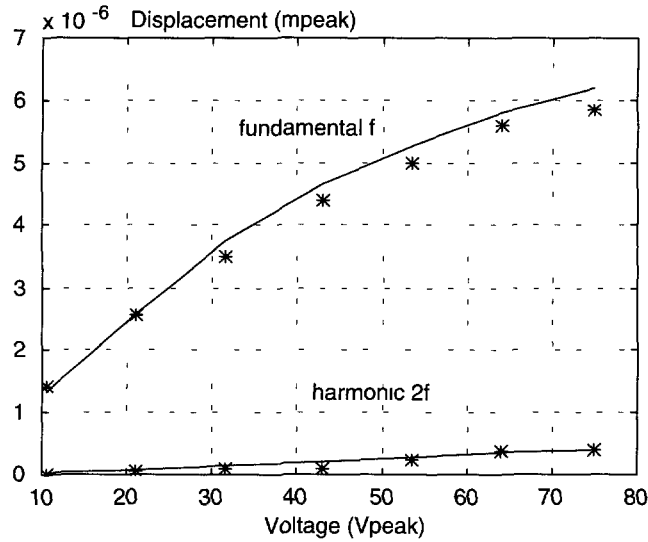


Fig. 10. — Displacement amplitude function of the applied voltage for the resonance working condition. (*) measurements, (—) simulations.

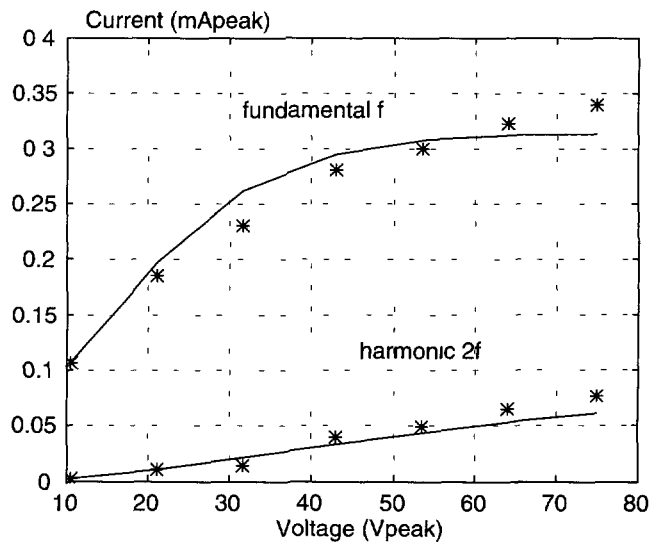


Fig. 11. — Current amplitude function of the applied voltage for the resonance working condition. (*) measurements, (—) simulations.

mode. We could say that the compressive stress creates a dipole opening and consequently relaxes the elasticity, while the extension stress tends to align all dipoles resulting in a material hardening [10].

It is commonly accepted that the saturation effect is related to the mechanical losses increase with the driving level [11, 12]. Our nonlinear model proposes a new interpretation. Indeed, the previous nonlinear simulations have shown that the saturation is linked to material

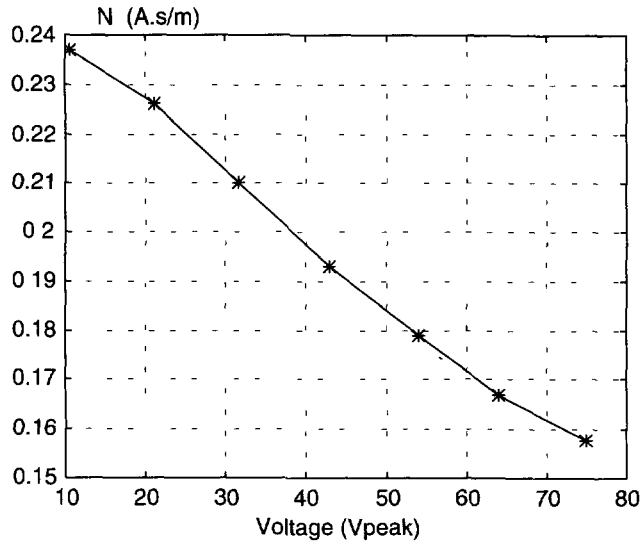


Fig. 12. — Simulated curve $N = f(\text{voltage})$

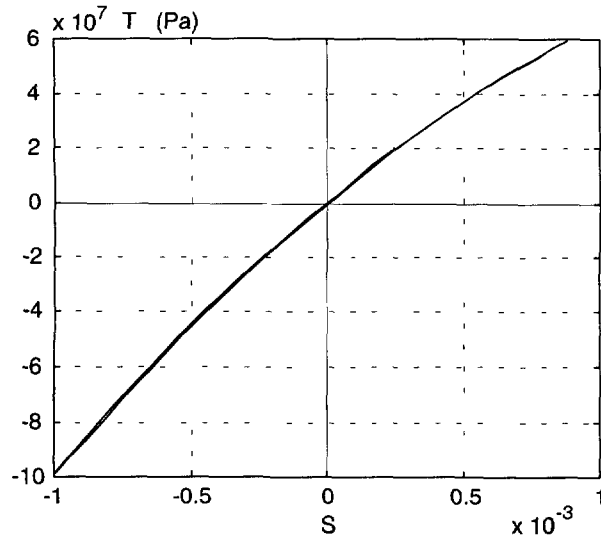


Fig. 13. — Simulated curve: stress = $f(\text{strain})$.

nonlinearities. To compare these two possible interpretations, a power signal analysis has been conducted by numerical simulations in both cases and compared after with experimental results.

The variation of the damping coefficient with the applied electrical field and the associated electrical power have been obtained by simulations. Nonlinear terms have been suppressed in all equations and the damping coefficient λ adjusted for each excitation level so as to retrieve the displacement amplitudes observed experimentally.

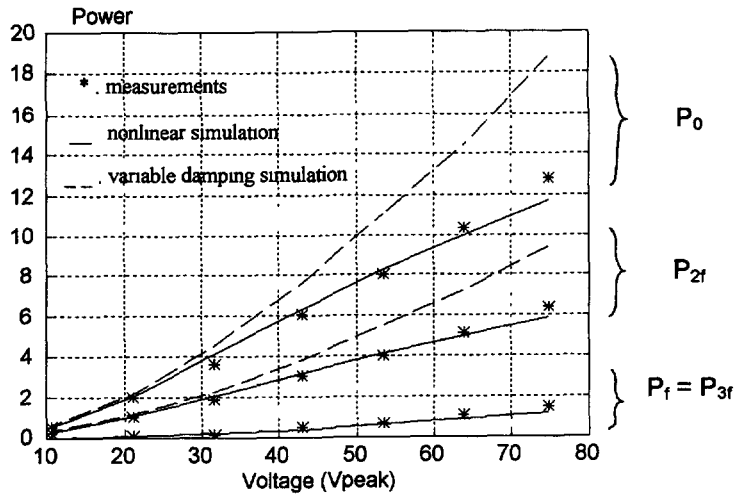


Fig 14. — Power curves

Figure 14 displays the different power curves:

- the measured power (represented as dots),
- the simulated power obtained with the variable damping, and without nonlinearities (represented as dashed lines),
- the simulated power obtained with nonlinear model, with a constant damping coefficient (represented as solid lines).

Figure 14 shows that the nonlinear approach leads to a better fit with the experimental data. The model with variable damping coefficient overestimates the power values and cannot explain the appearance of odd harmonics on the power signal.

Nonlinear terms have to be considered if one wants to estimate precisely the transducer performances.

5. Conclusion

For heavy duty Langevin sources, the nonlinear model gives a good interpretation of the transducer behavior. It explains especially the resonance frequency shift and hysteresis effects, the current and displacement saturation, the acoustical power saturation and the overtones generation.

Numerical simulations lead to nonlinear coefficients estimation that are important for the special working conditions of our transducer.

Acknowledgments

The authors are grateful to the CERDSM of Toulon, and especially to Dr D. Boucher, for supporting this research.

References

- [1] Landau L.D. and Lifshitz E.M., Mechanics, Course of theoretical physics, third edition, Pergamon, Vol.1, chapter V, pp. 58-95.
- [2] Meirovitch L., Elements of vibration analysis, Mechanical Engineering series, 2nd edition, chapter 9-10 (Mc Graw Hill International editions, 1986) pp. 347-407.
- [3] Shen Y.R., Principles of nonlinear Optics (Wiley Interscience, 1984).
- [4] Bloembergen N., Nonlinear Optics (Benjamin Inc., 1965).
- [5] Woollett R.S. and Le Blanc C.L., Ferroelectric nonlinearities in transducer ceramics, *IEEE Trans. Sonics and Ultrasonics* **SU20**, n°1, (January 1973) pp. 24-31.
- [6] Champ P., Modélisation et caractérisation sous haut niveau de sollicitation mécanique des céramiques piézoélectriques, Thèse Sci. (Institut National des Sciences Appliquées de Lyon, 1989) 265 pages.
- [7] Joshi S.P., Nonlinear constitutive relations for piezoceramic materials, *Smart. Mater. Struct.* **1** (1992) pp. 80-83.
- [8] Guyomar D., Aurelle N., Richard C., Gonnard P. and Eyraud L., Non linearities in Langevin transducers, in Proceedings of Ultrasonics International, Vol.2 (Novembre 1994) pp. 925-928.
- [9] Audigier D., Caractérisation de nouvelles céramiques de puissance du type PZT, fluorées, Thèse Sci. (Institut National des Sciences Appliquées de Lyon, 1996) 94 pages.
- [10] Cao H. and Evans A.G., Nonlinear deformation of ferroelectric ceramics, *J. Am. Ceram. Soc.* **76** (1993) 890-896.
- [11] Lubitz K. and Wersing W., Automatic performance testing of piezoelectric ceramics for power transducers, *Ferroelectrics* **40** (1982) 237-244.
- [12] Zug B., Étude des pertes d'origine piézoélectrique dans les matériaux piézoélectriques et les transducteurs ultrasonores, Thèse Sci. (Institut National des Sciences Appliquées de Lyon, 1994) 196 pages.